FEAT JOURNAL
FARM ENGINEERING AND AUTOMATION TECHNOLOGY JOURNAL
วารสารวิศวกรรมฟาร์มและเทคโนโลยีการควบคุมอัตโนมัติ

การออกแบบตัวควบคุมสไลด์ดิงโหมดชนิดติดตามแบบจำลองแบบไม่ต่อเนื่องและการประยุกต์ใช้กับระบบควบคุมตำแหน่งของมอเตอร์ซิงโครนัสที่คงทน

Design of a Discrete Sliding mode Model Following Controller and Application to a Synchronous Motor Robust Position Control System

Phongsak Phakamach[1)*] Udomvit Chaisakulkiet[2)] and Akharakit Chaithanakulwat[3)]

[1,2)] Rattanakosin International College of Creative Entrepreneurship,
Rajamangala University of Technology Rattanakosin, Thailand

[3)] Faculty of Science and Technology, Dhonburi Rajabhat University, Thailand

Received: 1 August 2024
Revised: 19 December 2024
Accepted: 19 December 2024
Available online: 26 December 2024

Abstract

In this paper, a Synchronous Motor position control system using a Discrete Sliding mode Model Following Control or DSMFC is presented to achieve accurate tracking in the presence of external load disturbances and plant parameter variations. The DSMFC algorithm uses the combination of model following control and sliding mode control to improve the dynamics response for command tracking. A design procedure is developed for determining the control function, the coefficients of the switching plane and the integral control gain. The control function is derived to guarantee the existence of a sliding mode. The chattering phenomenon is significantly reduced adopting the switching gain with the know parameters of the system. A DSP-based synchronous motor position control system using the DSMFC approach is illustrated. Experimental results indicated that DSMFC system performance

with respect to the sensitivity to parameter variations is greatly reduced. Also, its can achieve a rather accurate tracking and is fairly robust to load disturbances.

Keyword: Synchronous Motor: Robust Control: Sliding Mode Control: Model Following Control

* Corresponding author e-mail: pp2552@hotmail.com, phongsak.pha@rmutr.ac.th

1. Introduction

Recently, synchronous motors have been widely used as actuators for motion control and direct-drive applications especially in hostile environments. They have many advantages include higher torque/weight ratio, high torque capability, freedom of brush maintenance, lower rotor moment of inertia, better heat dissipation, long life operation, compact structure and lower weight as compared with DC motors and permanent magnet stator DC commutator motors having same output capacity[1]. The synchronous motor is preferable for certain high performance servo applications such as machine tools, industrial robots and aerospace actuators. The proposed scheme for a synchronous position control system, as shown in Fig. 1, consists of an inner loop for inverter switching and an outer loop for generating the command input. However, The dynamic position control of servo systems with unknown external load disturbances, and plant parameter variations are very complex and highly nonlinear. Moreover, the machine parameters (resistance and inductance) and load characteristics are not exactly known, which may vary during motor operation or processes with parametric uncertainty, where the conventional linear controller design may not assure satisfactory performances.

Variable Structure Control (VSC) or Sliding Mode Control (SMC) is invariant to system parameter variations and disturbances when the sliding mode occurs. Although the conventional VSC approach has been applied successfully in many applications [2-5], it cannot perform well in servo applications where the system is designed to track a command input. In order to improve tracking performance, the Integral Variable Structure Control or IVSC approach, presented in [6-7], combines an integral controller with the conventional VSC. The IVSC approach can eliminate the steady tracking error due to a step command input. However, IVSC yields the error when the system has to follow a changing command input, e.g., a ramp and sinusoidal inputs. Note that, this kind of input is generally encountered in servo applications. The Modified Integral Variable Structure Control or MIVSC approach, proposed in [8-9], uses a double integral action to solve this problem. Although,

the MIVSC method can give a better tracking performance than the IVSC method does at steady state, its performance during transient period needs to be improved.

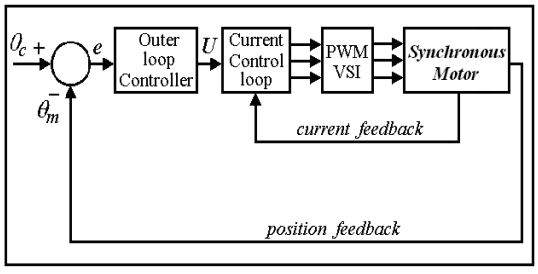

Figure 1 Block diagram of DSMFC synchronous motor position control systems.

The design and implementation of a synchronous motor position control systems using DSMFC approach is described. This approach, which is the extension of MIVSC approach and uses the feedforward path to improve the tracking performance, incorporates a model reference to improve the dynamics response for sinusoidal command tracking. The advantage of this approach is that the error trajectory in the sliding motion can be prescribed by the design. Also, it can achieve a rather accurate servo tracking and is fairly robust to plant parameter variations and external load disturbances. As a results, the tracking performance can be remarkably improved.

2. Design of DSMFC System

The structure of DSMFC system is shown in Fig. 2. It combines the conventional VSC with a double-integral compensator, a feedforward path from the input command, a reference model and a comparator.

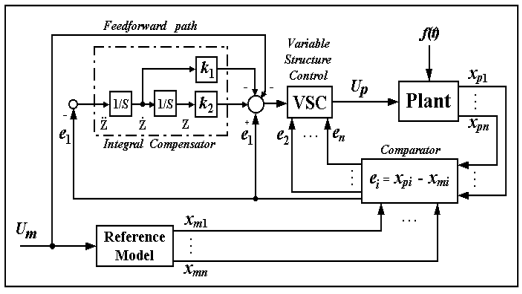

Figure 2 The structure of DSMFC system.

Let the plant be described by the following equation:

$$\dot{x}_{pi} = x_{p(i+1)} \;;i=1,\ldots,n\text{-}1, \dot{x}_{pn} = -\sum_{i=1}^{n} a_{pi} x_{pi} + b_p U_p - f(t) \quad (1)$$

where a_{pi} and b_p are the plant parameters; $f(t)$ are disturbances; U_p is the control input of the plant.

The reference model is represented by

$$\dot{x}_{mi} = x_{m(i+1)} \;;i=1,\ldots,n\text{-}1, \; \dot{x}_{mn} = -\sum_{i=1}^{n} a_{mi} x_{mi} + b_m U_m \quad (2)$$

where U_m is the input command of the system.

Defining $e_i = x_{pi} - x_{mi} \;;(i=1,\ldots,n)$ and subtracting (2) from (1), the error differential equation is

$$\dot{e}_i = e_{i+1} \;;i=1,\ldots,n\text{-}1,$$
$$\dot{e}_n = -\sum_{i=1}^{n} a_{pi} e_i - \sum_{i=1}^{n} (a_{mi} - a_{pi}) x_{mi} + b_m U_m - b_p U_p - f(t). \quad (3)$$

Using the SMFC approach [9, 14] to the error dynamics in order to synthesize the control signal, U_p and assuming the asymptotic divergence of the error to zero, the DSMFC system in Fig. 2 can be described as

$$\ddot{z} = -e_1, \dot{e}_i = e_{i+1}; i=1,\ldots,n\text{-}1,$$
$$\dot{e}_n = -\sum_{i=1}^{n} a_{pi} e_i - \sum_{i=1}^{n} (a_{mi} - a_{pi}) x_{mi} + b_m U_m - b_p U_p - f(t) \quad (4)$$

where U_p is the control function.

Consider the discretization of the system given in (4). If the derivative is approximated by the forward difference as [10]

$$\dot{e}_i(t) = \frac{e_i(t+T) - e_i(t)}{T} \quad (5)$$

where T is the sampling interval, then the discretized version of the system (4) can be represented as:

$$\dot{z}(k+1) = \dot{z}(k) - Te_1(k) \quad (5a)$$

$$e_i(k+1) = e_i(k) + Te_{i+1}(k) \;; i=1,\ldots,n\text{-}1 \quad (5b)$$

$$\dot{e}_n(k+1) = e_n(k) - T\sum_{i=1}^{n} a_{pi} e_i - T\sum_{i=1}^{n} (a_{mi} - a_{pi}) x_{mi}(k) + Tb_m U_m(k) - Tb_p U_p(k) - Tf(k) \quad (5c)$$

The switching function, σ is given by

$$\sigma(k) = c_1[e_1(k) - K_1\dot{z}(k) - K_2 z(k) - r(k)] + \sum_{i=2}^{n} c_i e_i(k) \quad (6)$$
$$; C_i > 0 = \text{constant}, C_n = 1.$$

In the discrete variable structure control system, the control input is computed at discrete instants and applied to the system during the sampling interval so that an ideal sliding motion cannot be obtained [11-12]. The conditions ensuring the existence and reachability of a nonideal sliding motion are:

$$\sigma(k)\Delta\sigma(k+1) < 0 \quad (7a)$$

$$|\Delta\sigma(k+1)| < \frac{\xi}{2} \quad (7b)$$

where $\Delta\sigma(k+1) = \sigma(k+1)$; $\sigma(k)$ and ξ is a small positive number. The control function can be chosen to guarantee that the inequalities (7) are satisfied, so a sliding mode motion control within the range of ξ will appear or $\sigma(k) < \xi$.

Design of such a system involves (1) the choice of the control function $U_p(k)$ to guarantee the existence of a sliding mode control, (2) the determination of the switching function $\sigma(k)$ and the integral control gain K_I such that the system has the desired properties and (3) the elimination of chattering phenomena of the control input by using the smoothing function.

A. Choice of control function

The control signal can be determined as follows. From (5) and (6) [13], we have

$$\Delta\sigma(k+1) = -Tc_1(K_1\ddot{z}(k) + K_2\dot{z}(k)) + T\sum_{i=2}^{n} c_{i-1} e_i - \sum_{i=1}^{n} a_{pi} e_i(k) + \sum_{i=1}^{n} (a_{mi} - a_{pi}) x_{mi}(k) - Tb_m U_m(k) + Tb_p U_p(k) - Tf(k) \quad (8)$$

Let $a_{pi} = a_{pi}^0 + \Delta a_{pi}$; $i = 1,\ldots,n$

and $b_p = b_p^0 + \Delta b_p$; $b_p^0 > 0$, $\Delta b_p > -b_p^0$

where a_{pi}^0 and b_p^0 are nominal values;

Δa_{pi} and Δb_p are the associated variations.

Let the control function $U_p(k)$ be decomposed into

$$U_p(k) = U_{eq}(k) + U_s(k) \tag{9}$$

where the so called equivalent control $U_{eq}(k)$ is defined as the solution of (9) under the condition where there is no disturbances and no parameter variations, that is $\Delta\sigma(k+1) = 0$, $f(k)=0$, $a_{pi}=a_{pi}^0$, $b_p=b_p^0$ and $U_p(k)= U_{eq}(k)$.

This condition results in

$$U_{eq}(k) = \left\{ -c_1(K_1\ddot{z}(k) + K_2\dot{z}(k)) - \sum_{i-2}^{n-1} c_{i-1}e_i(k) + \sum_{i=1}^{n-1} a_{pi}^0 e_i(k) - \sum_{i=1}^{n}(a_{mi} - a_{pi})x_{mi}(k) + b_m U_m(k) \right\} / b_p^0 \tag{10}$$

In the sliding motion, $\sigma(k) = 0$, one can obtain

$$e_n(k) = \left[-c_1[e_1(k) - K_1\dot{z}(k) - K_2 z(k) - r(k)] - \sum_{i=2}^{n} c_i e_i(k) \right] \tag{11}$$

Substitution of (11) into (10) yields

$$\begin{aligned} U_{eq}(k) = \Big\{ & -c_1(K_1\ddot{z}(k) + K_2\dot{z}(k)) - T\sum_{i-2}^{n-1} c_{i-1}e_i(k) + T\sum_{i=1}^{n-1} a_{pi}^0 e_i(k) \\ & - T\sum_{i=1}^{n}(a_{mi} - a_{pi})x_{mi}(k) + b_m U_m(k) \\ & + (c_{i-1} - a_{pn}^0)\big[c_1(e_1(k) - K_1\dot{z}(k) + K_2 z(k) - U_m(k)) \\ & + \sum_{i=2}^{n-1} c_i e_i(k)\big] \Big\} / b_p^0 \end{aligned} \tag{12}$$

The function $U_s(k)$, is employed to eliminate the influence due to Δa_{pi}, Δb_p and $f(k)$ so as to guarantee the existence of a sliding mode control, is constructed as

It is required to guarantee the existence of the sliding mode. This function is constructed as

$$U_s(k) = \varphi_1(e_1(k) - K_1\ddot{z}(k) - K_2 z(k) - U_m(k)) + T\sum_{i=2}^{n} \varphi_i e_i(k) + \varphi_{n+1}. \tag{13}$$

Where :

$$\varphi_1 = \begin{cases} \alpha_1 & \text{if } [e_1(k) - K_1\dot{z}(k) - K_2 z(k) - U_m(k)]\sigma(k) \rangle 0 \\ \beta_1 & \text{if } [e_1(k) - K_1\dot{z}(k) - K_2 z(k) - U_m(k)]\sigma(k) \langle 0 \end{cases}$$

$$\varphi_i = \begin{cases} \alpha_i & \text{if } e_i\sigma(k) \rangle 0 \\ \beta_i & \text{if } e_i\sigma(k) \langle 0 \end{cases} \quad ,i = 2,\ldots,n \text{ and}$$

$$\varphi_{n+1} = \begin{cases} \alpha_{n+1} & \text{if } \sigma(k) \rangle 0 \\ \beta_{n+1} & \text{if } \sigma(k) \langle 0 \end{cases}.$$

Substitute (7) and (9) into (6), to obtain

$$\begin{aligned} & \Delta\sigma(k+1)\sigma(k) = \\ & T\{ [-\Delta a_{p1} + a_{p1}^0 \Delta b_p / b_p^0 + c_1(c_{n-1} - a_{pn}^0)(1 + \Delta b_p / b_p^0) + b_p\varphi_1] \\ & (e_1(k) - K_1\dot{z}(k) - K_2 z(k) - U_m(k))\sigma(k) \\ & + \sum_{i=2}^{n-1}\{[-\Delta a_{pi} + a_{pi}^0 \Delta b_p / b_p^0 - c_{i-1}\Delta b_p / b_p^0 + c_i(c_{n-1} - a_{pn}^0)(1 + \Delta b_p / b_p^0) + b_p\Psi_i]e_i(k)\sigma(k)\} \\ & + [-\Delta a_{pn} + (c_{n-1} - a_{pn}^0) + b_p\Psi_n]e_n\sigma(k) \quad + [N(k) + b_p\Psi_{n+1}]\sigma(k) \end{aligned} \tag{14}$$

Where

$$\begin{aligned} N = & -(K_1\dot{z}(k) + K_2 z(k))(\Delta a_{p1} - a_{p1}^0 \Delta b_p / b_p^0) + \Delta b_p / b_p^0 [c_1(K_1\ddot{z}(k) + K_2\dot{z}(k))] \\ & + [-\sum_{i=1}^{n}(a_{mi} - a_{pi}^0)x_{mi}(k) + b_m U_m]\Delta b_p / b_p^0 - f(k). \end{aligned}$$

In order for (7) to be satisfied, the following conditions must be met,

$$\varphi_i = \begin{cases} \alpha_i \ \langle\ \varphi\mathrm{L}_i = \mathrm{Inf}[\Delta a_{pi} - a_{pi}^0 \Delta b_p / b_p^0 + c_{i-1}\Delta b_p / b_p^0 \\ \quad - c_i(c_{n-1} - a_{pn}^0)(1 + \Delta b_p / b_p^0)] / b_p \\ \beta_i \ \rangle\ \varphi\mathrm{U}_i = \mathrm{Sup}[\Delta a_{pi} - a_{pi}^0 \Delta b_p / b_p^0 + c_{i-1}\Delta b_p / b_p^0 \\ \quad - c_i(c_{n-1} - a_{pn}^0)(1 + \Delta b_p / b_p^0)] / b_p \end{cases} \tag{15a}$$

where $i=1,\ldots,n-1$, $c_0 = 0$

$$\varphi_n = \begin{cases} \alpha_n \ \langle\ \varphi\mathrm{L}_i = \mathrm{Inf}[\Delta a_{pn} + a_{pn}^0 - c_{n-1}] / b_p \\ \beta_n \ \rangle\ \varphi\mathrm{U}_i = \mathrm{Sup}[\Delta a_{pn} + a_{pn}^0 - c_{n-1}] / b_p \end{cases} \tag{15b}$$

and $$\varphi_{n+1} = \begin{cases} \alpha_{n+1} \ \langle\ \varphi\mathrm{L}_{(n+1)} = \mathrm{Inf}[-N(k)] / b_p \\ \beta_{n+1} \ \rangle\ \varphi\mathrm{U}_{(n+1)} = \mathrm{Sup}[-N(k)] / b_p \end{cases}. \tag{15c}$$

For satisfying (7), if the sampling interval T is enough small, one can be obtain:

$$L_1\langle\varphi_1\langle M_1, \quad L_i\langle\varphi_i\langle M_i \quad ;i = 2,\ldots,n\text{-}1 \tag{16a}$$

$$L_n\langle\varphi_n\langle M_n, \quad L_{n+1}\langle\varphi_{n+1}\langle M_{n+1} \tag{16b}$$

where:

$$M_1 = \inf\left\{[\Delta a_{p1} - a_{p1}^0\Delta b_p / b_p^0 + c_{i-1}\Delta b_p / b_p^0 - c_1(c_{n-1} - a_{pn}^0)(1+\Delta b_p / b_p^0) + \gamma_1 / (T|e_1(k) - K_1\dot{z}(k) - K_2 z(k) - U_m(k)|)]/ b_p\right|$$

$$L_1 = \sup\left\{[\Delta a_{p1} - a_{p1}^0\Delta b_p / b_p^0 + c_{i-1}\Delta b_p / b_p^0 - c_1(c_{n-1} - a_{pn}^0)(1+\Delta b_p / b_p^0) - \gamma_1 / (T|e_1(k) - K_1\dot{z}(k) - K_2 z(k) - U_m(k)|)]/ b_p\right|$$

$$M_i = \inf\left\{[\Delta a_{pi} - a_{pi}^0\Delta b_p / b_p^0 + c_{i-1}\Delta b_p / b_p^0 - c_i(c_{n-1} - a_{pn}^0)(1+\Delta b_p / b_p^0) + \gamma_1 / (T|x_i(k)|)]/ b_p\right|$$

$$L_i = \sup\left\{[\Delta a_{pi} - a_{pi}^0\Delta b_p / b_p^0 + c_{i-1}\Delta b_p / b_p^0 - c_i(c_{n-1} - a_{pn}^0)(1+\Delta b_p / b_p^0) - \gamma_1 / (T|x_i(k)|)]/ b_p\right|$$

$$M_n = \inf\left\{[\Delta a_{pn} - a_{pn}^0 - c_{n-1} + \gamma_n / (T|e_n(k)|)]/ b_p\right.$$

$$L_n = \sup\left\{[\Delta a_{pn} - a_{pn}^0 - c_{n-1} - \gamma_n / (T|e_n(k)|)]/ b_p\right.$$

$$M_{n+1} = \inf\left\{N(k) + \gamma_{n+1} / T]/ b_p\right. \text{ and}$$

$$L_{n+1} = \sup\left\{N(k) - \gamma_{n+1} / T]/ b_p\right.$$

in which γ_i ;i=1,…,n+1, are positive constants and

$\gamma_1 + \cdots + \gamma_{n+1} < \xi / 2$.

From (15) and (16), if the T is enough small, one can obtain the bound of α_i and β_i as :

$$L_i < \alpha_i < \varphi L_i \quad \varphi U_i < \beta_i < M_i \quad ,i = 1,\ldots,n+1. \tag{17}$$

If φ_i ,i=1,…,n+1, are chosen as $\varphi_i < \alpha_i < -\beta_i$ finally, the control can be represented as

$$\begin{aligned} U_p = \Big\{ & -c_1(K_1\ddot{z}(k) + K_2\dot{z}(k)) - \sum_{i=2}^{n-1} c_{i-1}e_i(k) + \sum_{i=1}^{n-1} a_{pi}^0 e_i(k) \\ & - \sum_{i=1}^{n}(a_{mi} - a_{pi}^0)x_{mi}(k) + b_m U_m(k) + (c_{n-1} - a_{pn}^0) \\ & \left[c_1(e_1(k) - K_1\dot{z}(k) - K_2 z(k) - U_m(k)) + \sum_{i=2}^{n-1} c_i e_i(k)\right]\Big\} / b_p^0 \\ & + \left(\varphi_1|e_1(k) - K_1\dot{z}(k) - K_2 z(k) - U_m(k)| + \sum_{i=2}^{n}\varphi_i|e_i(k)| \right. \\ & \left. + \varphi_{n+1}\right) sign(\sigma(k)). \end{aligned} \tag{18}$$

From (17), the upper and low bounds of the φ_i, can be obtain

$$\hat{L}_i < \hat{\varphi}_i < \hat{M}_i \quad ,i=1,\ldots,n+1 \tag{19}$$

Where $\hat{M}_i = -\max(|\varphi L_i|, |\varphi U_i|)$ and $\hat{L}_i = -\max(|L_i|, |M_i|)$

B. Determination of switching plane and integral control gain

In the above subsection it has been proved that if the solution of the ideal sliding motion is asymptotically stable, it will close to the solution of the non-ideal sliding within the range of ξ. Thus one can choose the switching plane and integral control gain of the basis of the ideal sliding motion. While in the ideal sliding motion, the system can described by (4) can be reduced to [14-15]:

$$\dot{z}(k+1) = \dot{z}(k) - Te_1(k) \tag{20a}$$

$$e_i(k+1) = e_i(k) + Te_{i+1}(k) \quad ;i=1,\ldots,n\text{-}2 \tag{20b}$$

$$\dot{e}_n(k+1) = e_{n-1}(k) - T[C_1K_1\dot{z}(k) - C_2K_2z(k)] - \sum_{i=1}^{n} a_{pi}e_i(k) \tag{20c}$$

The characteristic equation when the system is on the sliding surface can be shown as

$$H(s) = \frac{E_1(z)}{U_m(z)} = \frac{\left(\frac{z-1}{T}\right)^2 c_1}{\left(\frac{z-1}{T}\right)^n + c_{n-1}\left(\frac{z-1}{T}\right)^{n-1} + \ldots + c_1K_1\left(\frac{z-1}{T}\right) + c_1K_2}. \tag{21}$$

The characteristic equation of the system (21) is

$$\left(\frac{z-1}{T}\right)^n + c_{n-1}\left(\frac{z-1}{T}\right)^{n-1} + \ldots + c_1K_1\left(\frac{z-1}{T}\right) + c_1K_2 = 0 \tag{22}$$

Since this characteristic equation is independent of the plant parameter, the DSMFC approach is robust to plant parameter variations. Further, one can choose the coefficients of the switching function and the integral control gain by the pole assignment technique such that this sliding motion has desirable properties [13].

Let $z\text{-}1/T = \eta$. Then (22) can be rewritten as

$$\eta^n + C_{n-1}\eta^{n-1} + \ldots + C_1K_1\eta + C_2K_2 = 0 \qquad (23)$$

The transient response of the system can be determined by suitably selecting the poles of the transfer function (21).

$$\text{Let} \quad \eta^n + \alpha_1\eta^{n-1} + \ldots + \alpha_{n-1}\eta + \alpha_n = 0 \qquad (24)$$

be the desired characteristic equation (closed-loop poles), the coefficient C_1, C_2 and K_1, K_2 can be obtained by

$$C_{n-1} = \alpha_1\,,\ C_1 = \alpha_{n-2}\,,\ K_1 = \alpha_{n-1}/C_1 \text{ and } K_2 = \alpha_n/C_1.$$

C. Chattering Considerations

Normally, the sign function sign (σ) given by (18), will give rise to chattering in the control signal. In order to reduce the chattering, the sign function can be replaced by the continuous function [13], given by

$$M_\delta(\sigma) = \frac{\sigma(k)}{|\sigma(k)| + \delta_0 + \delta_1|\ddot{z}(k)|} \qquad (25)$$

where $\delta = \delta_0 + \delta_1|\ddot{z}(k)|$; δ_0 and δ_1 are positive constants.

3. Dynamics modeling of synchronous motor

The synchronous motor considered is a 3-phase permanent magnet synchronous motor with sinusoidal back electromotive force (EMF) as shown in Fig. 3. The stator windings are identical, displaced by 120 degrees and sinusoidally distributed. The voltage equation for the stator windings can be expressed as

$$\begin{bmatrix} v_{as} \\ v_{bs} \\ v_{cs} \end{bmatrix} = \begin{bmatrix} R_s & 0 & 0 \\ 0 & R_s & 0 \\ 0 & 0 & R_s \end{bmatrix} \begin{bmatrix} i_{as} \\ i_{bs} \\ i_{cs} \end{bmatrix} + \frac{d}{dt} \begin{bmatrix} L_s & 0 & 0 \\ 0 & L_s & 0 \\ 0 & 0 & L_s \end{bmatrix} \begin{bmatrix} i_{as} \\ i_{bs} \\ i_{cs} \end{bmatrix} + \omega_r k_e \begin{bmatrix} \sin(\theta_r) \\ \sin(\theta_r - 2\pi/3) \\ \sin(\theta_r + 2\pi/3) \end{bmatrix} \qquad (26)$$

where

v_{as}, v_{bs}, v_{cs} is the applied stator voltage;

i_{as}, i_{bs}, i_{cs} is the applied stator currents;

R_s is the resistance of each stator winding;

L_s is the inductance of the stator winding;

ω_r is the electrical motor angular velocity;

θ_r is the electrical rotor angular displacement and

k_e is the voltage constant.

The electromagnetic torque can be expressed as

$$T_e = k_t\left[i_{as}\sin(\theta_r) + i_{bs}\sin\left(\theta_r - \frac{2\pi}{3}\right) + i_{cs}\sin\left(\theta_r + \frac{2\pi}{3}\right)\right] \qquad (27)$$

where k_t is the current constant and

P is number of pole.

The torque, velocity and position may be related by

$$T_e = J_m\left(\frac{2}{P}\right)\frac{d\omega_r}{dt} + B_m\left(\frac{2}{P}\right)\omega_r + T_L \quad (28a)$$

$$\theta_r = \int \omega_r dt \quad (28b)$$

$$\omega_m = \omega_r\left(\frac{2}{P}\right) \quad (28c)$$

where J_m is the inertia of the rotor;

B_m is the damping coefficient;

T_L is the load torque and

θ_m is the mechanical angular position of rotor.

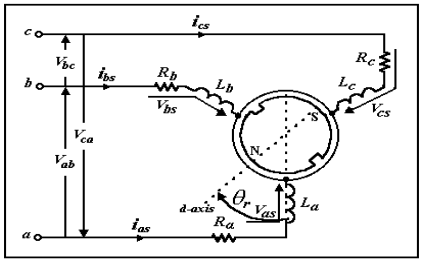

Figure 3 The synchronous motor modeling.

A motor driver is a sinusoidal current controlled pulse width modulation (PWM) voltage source inverter (VSI) as shown in Fig. 4, consisting of the DC-SIN transform, current compensator and PWM-VSI circuits. The mode of the PWM-VSI circuit can be simplified as a constant gain K_A=V_{dc}/2E_d where V_{dc} is the DC supply voltage in the VSI and E_d are the triangular peak values in the PWM.

The current loop is designed to achieve fast and accurate current tracking. In this condition, the mode of the current-controlled loop can be simplified to a single- input single-output (SISO) system as shown in Fig. 5, where K_A and g_I are the constants relating to the inverter and the current control loop.

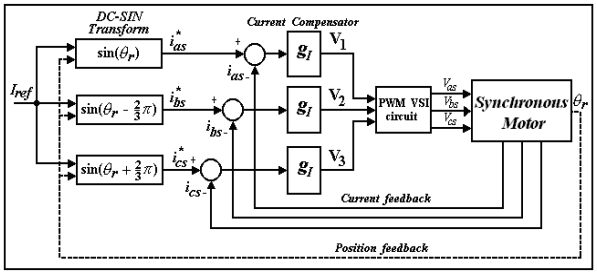

Figure 4 The current-controlled PWM-VSI.

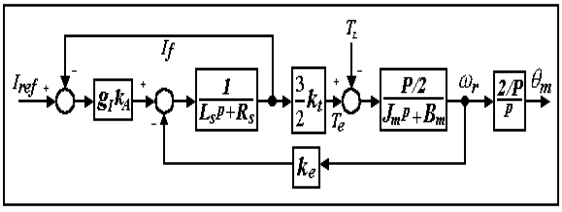

Figure 5 Dynamic SISO model of the synchronous motor.

4. The design of DSMFC system for position control of synchronous motor

The implementation of DSMFC system is shown in Fig. 6 and its block diagram is shown in Fig. 7. The system contains a synchronous motor, a power circuit driver and the DSMFC. The parameters of the synchronous motor and the DSMFC controller are shown in Table 1 and Table 2, respectively.

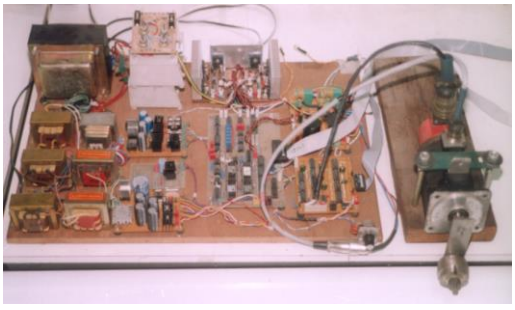

Figure 6 The synchronous motor with DSMFC.

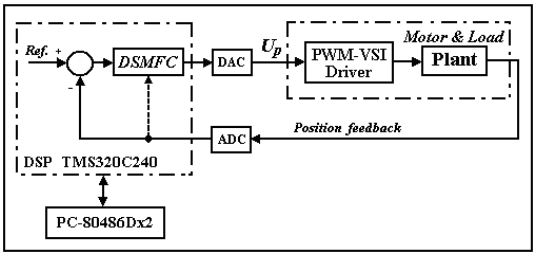

Figure 7 The DSMFC for the synchronous motor system.

The simplified dynamic model of the synchronous motor for position control can be described as

$$\dot{x}_{p1} = x_{p2},\ \dot{x}_{p2} = x_{p3},\ \dot{x}_{p3} = -a_{p1}x_{p1} - a_{p2}x_{p2} - a_{p3}x_{p3} + b_p U_p - \dot{f}(t) \tag{29}$$

where $a_{p1} = 0$, $a_{p2} = \dfrac{(R_s + g_I k_A)B_m + \frac{3}{4}Pk_t k_e}{L_s J_m}$,

$a_{p3} = \dfrac{(R_s + g_I k_A)}{L_s} + \dfrac{B_m}{J_m}$, $b_p = \dfrac{(\frac{3}{2} g_I k_A k_t)}{L_s J_m}$ and

$f(t) = \dfrac{(R_s + g_I k_A)}{J_m L_s} T_L + \dfrac{1}{J_m}\dot{T}_L$ and where

$x_{p1} = \theta_m$ is the mechanical angular angle of the rotor;

$U_m = \theta_c$ is desired position and

U_P is the control input of the plant.

The reference model is chosen as

$$\dot{x}_{m1} = x_{m2},\ \dot{x}_{m2} = x_{m3},\ \dot{x}_{m3} = -a_{m1}x_{m1} - a_{m2}x_{m2} - a_{m3}x_{m3} + b_m U_m . \tag{30}$$

Defining $e_i = x_{pi} - x_{mi}$;(i= 1,2,3), the DSMFC system can be represented as

$$\dot{z}(k+1) = \dot{z}(k) - Te_1(k) \tag{31a}$$

$$e_2(k+1) = e_2(k) + Te_3(k) \ ;i=1,\ldots,n\text{-}1 \tag{31b}$$

$$e_3(k+1) = e_3(k) - T\sum_{i=1}^{n} a_{pi}e_i(k) - T\sum_{i=1}^{n}(a_{mi} - a_{pi})x_{mi}(k) + Tb_m U_m(k) - Tb_p U_p(k) - Tf(k) \tag{31c}$$

Following the design procedure we have the control law to implement as

$$\begin{aligned} U_P(k) = \{ & c_1(K_1\ddot{z}(k) + K_2\dot{z}(k)) + a_{p1}^0 e_1(k) + a_{p2}^0 e_2(k) - [(a_{m1} - a_{p1}^0)x_{m1}(k) \\ & + (a_{m2} - a_{p2}^0)x_{m2}(k) + (a_{m3} - a_{p3}^0)x_{m3}(k) + b_m U_m)] \\ & + (c_2 - a_3^0)[c_1(e_1(k) - K_1\dot{z}(k) - K_2 z(k) - r(k)) + c_2 e_2(k)]\}/b^0 \\ & + (\Psi_1|e_1(k) - K_1\dot{z}(k) - K_2 z(k) - r(k)| + \Psi_2|e_2(k)| \\ & + \Psi_3|e_3(k)| + \Psi_4)M_\delta(\sigma) \end{aligned} \tag{32}$$

The switching function, $\sigma(k)$ from (6), is given by

$$\sigma(k) = c_1(e_1(k) - K_1\dot{z}(k) - K_2 z(k) - r(k)) + c_2 e_2(k) + e_3(k) \tag{33}$$

Table 1.

Parameter of the synchronous motor

Parameter	Value	Dimension
P	4	*pole*
R_s	0.8	Ω
L_s	0.005	*H*
K_A	6	*dimensionless*
g_I	4.5	*dimensionless*
B_m	0.000	*N-m/s*
J_m	0.00016	*Kg-m*^{2}
K_e	0.178	*V-s/rad*
K_t	0.182	*N-m/A*

Table 2.

Parameters of the DSMFC controller

Parameter	Value
λ_1, λ_2	-20.14±32.78i
λ_3, λ_4	-32.58, -18.95
C_1, C_2	1,895.48, 125.27
K_1, K_2	42.38, 84.63
φ_1, φ_2	-1, -0.1
φ_3, φ_4	-0.0005, -0.001
a_{m1}, a_{m2}	15,000, 1,320
a_{m3}, b_m	52, 15,000
$a_{p2}{}^0, a_{p3}{}^0$	13,725.26, 2,684
$b_p{}^0$	63,426.97
δ_0, δ_1	1, 150

5. Experimental results and discussion

The experimental results of the dynamic response are plotted in Fig. 8 and Fig. 9. In order to evaluate the tracking performance of the DSMFC approach for both steady and transient periods, a sinusoidal command is first introduced for certain period of time before it is changed abruptly to a constant value. In addition the results are compared with those obtained from MIVSC and IVSC approaches under the same testing conditions. It is clear from the figures that the DSMFC can follow the command input extremely well during steady state as well as transient periods. That is, it converges very fast to zero but the other give rise to steady state errors. Although MIVSC seems to track well during the steady state of the sinusoidal command input, it gives a noticeable overshoot an tracking error during the input change. Among them, IVSC performs poorly, it gives a substantially sustained tracking error. Furthermore, experimental results demonstrate that the developed DSMFC scheme has a much better performance related to reduction in steady state error, faster settling time, smaller overshoot in the position response and much better disturbance rejection capabilities.

6. Conclusions

In this paper, the DSMFC approach is explained and presented. It exhibits good feature of the conventional IVSC and MIVSC controller, such as better performance to reduction in steady state error, faster settling time, smaller overshoot in the position response, robustness in the face of model error and parameter variations. The application of DSMFC to the synchronous motor position control system has illustrated that the DSMFC method can improve the tracking performance by 72% and 86% when compared to the MIVSC and IVSC approaches, respectively.

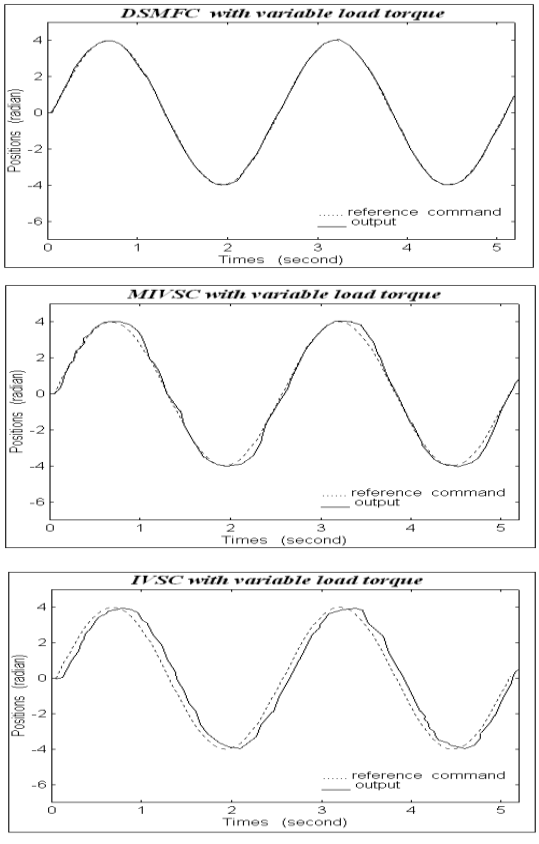

Figure 8 Comparison of ramp position tracking

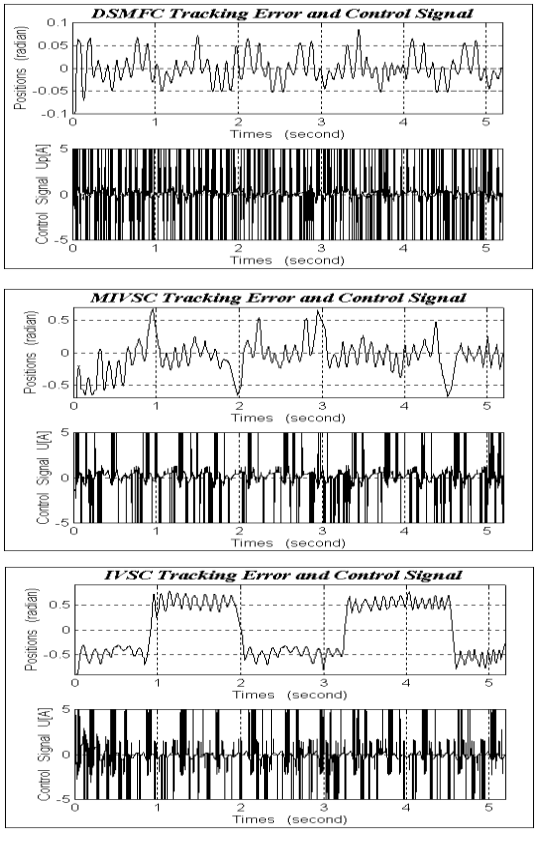

Figure 9 Comparison of position tracking errors and control signal.

7. Acknowledgements

Authors of the paper would like to acknowledge the support of Rattanakosin International College of Creative Entrepreneurship, Rajamangala University of Technology Rattanakosin, Thailand.

8. References

[1] Dote Y, Kinoshita S. Brushless Servomotors Fundamental and Applications. Clarendon Press Oxford: 1990.

[2] Utkin VI, Guldner J, Shi J. Sliding Mode Control in Electromechanical Systems. Taylor & Francis: London; 1999.

[3] John HY, Weibing G, James CH. Variable Structure Control. IEEE Transaction on Industrial Electronics. 1993; 40(1): 1-22.

[4] Komurcugil H, Biricik S, Bayhan S, Zhang Z. Sliding Mode Control: Overview of Its Applications in Power Converters. IEEE Industrial Electronics Magazine. 2021; 15(1): 40-49.

[5] Wu L, Liu J, Vazquez S, Mazumder S.K. Sliding Mode Control in Power Converters and Drives: A Review. IEEE/CAA Journal of Automatica Sinica. 2022; 9(3): 392-406.

[6] Chern TL, Wong J. DSP-Based Integral Variable Structure Control for DC Motor Servo Drivers. IEE Proc. Control Theory Applications. 1995; 142(5): 444-50.

[7] Chern TL, Chang J. DSP-Based Induction Motor Drivers Using Integral Variable Structure Model Following Control Approach. IEEE International Electric Machine and Drives Conference Record. 1997; 20: 9.1-9.3.

[8] Nungam S, Daungkua P. Modified Integral Variable Structure Control for Brushless DC Servomotor. 21st Electrical Engineering Conference, Thailand. Nov. 1998; 138-41.

[9] Worapongpat N, Phakamach P, Chaisakulkiet U. A Flexible Arm Manipulator Control System Using Modified Discrete Sliding mode Model Following Controller with Sinusoidal Command Input. UTK Journal. 2020; 14(1): 14-22.

[10] Philips CI, Nagle HT. Digital Control System Analysis and Design. Pearson; 4th edition, International Edition: 2014.

[11] Joseph E. Comparison of Sliding Mode and Proportional Integral Control for Brushless DC Motor. International Journal of Engineering Sciences & Research Technology. 2016; 5(8): 372-378.

[12] Dursun EH, Durdu A. Speed Control of a DC Motor with Variable Load Using Sliding Mode Control. International Journal of Computer and Electrical Engineering. 2016; 8(30): 219-226.

[13] Phakamach P. A Variable Structure Control Based on Fuzzy Logic Algorithm with an Integral Compensation for a DC Servomotor Drives. The International MultiConference of Engineers and Computer Scientists. Hong Kong. 2007.

[14] Phakamach P. Development of a Discrete Sliding mode Model Following Control for an Automatic Voltage Regulator Control Systems. International Congress on Natural Sciences and Engineering (ICNSE'2014), Kyoto, Japan. 2014.

[15] Phakamach P, Chaisakulkiet U, Wachirawongpaisarn S. Robust Tracking Control Scheme for a Ship Maneuvering with Uncertain Dynamics Using Modified Fuzzy Logic Variable Structure Controller Approach. Farm Engineering and Automation Technology Journal. 2022; 9(1): 27-38.